Effect of elastic interactions on the self-assembly of multiferroic nanostructures in epitaxial films

Julia Slutsker,[1] Igor Levin,[1] Jianhua Li,[2] Andrei Artemev,[3] and Alexander L. Roytburd[2]

[1]*Ceramics Division, National Institute of Standards and Technology, Gaithersburg, Maryland 20899, USA*
[2]*Materials Science and Engineering Department, University of Maryland, College Park, Maryland 20742, USA*
[3]*Department of Mechanical and Aerospace Engineering, Carleton University, Ottawa, ON K1S 5B6, Canada*

Combined theoretical and experimental studies of self-assembled multiferroic nanostructures in epitaxial films reveal the dominant role of elastic interactions, caused by epitaxial stresses, in defining the morphology of the nanostructures. The phase field model, which considered the individual phases in the film as elastic domains, has predicted successfully the complex morphologies observed in epitaxial multiferroic $CoFe_2O_4$-$PbTiO_3$ films grown on $SrTiO_3$ substrates with {001}, {110}, and {111} orientations. It is shown that nanostructures containing isolated magnetic nanorods in a ferroelectric matrix or vice versa can be obtained by varying the substrate orientation and phase fraction.

PACS number(s): 81.07.−b, 81.05.Zx, 77.84.Dy, 81.16.Dn

The self-assembly of multiphase nanostructures in epitaxial films attracts considerable interest because such composite thin films can exhibit a variety of coupled functional responses depending on the nature of the constituent phases.[1–7] For example, multiferroic nanostructures, composed of ferroelectric (FE) and ferromagnetic (FM) phases can change either polarization in response to the magnetic field or magnetization in response to the electric field. In[1] a self-assembled nanostructure consisting of $BaTiO_3$ and $CoFe_2O_4$ phases on $SrTiO_3$ substrate with epitaxial relations between them has been manufactured. It had been shown that due to the elastic interaction between the phases, the paraelectric/ferroelectric transition in $BaTiO_3$ leads to the change of magnetization of $CoFe_2O_4$. It can be expected that the strong elastic interaction between nanophases in epitaxial films enhances magnetization/polarization coupling compared to laminated ceramic composites.[8–10]

In this paper, we present a thermodynamic theory, phase-field modeling, and experimental observations which demonstrate that elastic interactions not only control the magnetic and electric responses of the self-assembled multiferroic nanostructures in epitaxial films, but also dictate their architectures. We assume that the morphology of the nanostructure is determined by the minimum of the elastic energy of epitaxial stresses which arise due to a nanoscale of component phases. Thus, the individual phases in the nanostructure can be considered as elastic domains which self-assemble to minimize the long-range elastic field in the film.[11,12] We use this approach to develop a phase-field model for the analysis and prediction of morphologies and stress conditions in the two-phase nanostructures in constrained epitaxial layers. Several phase-field studies of a diffusion-controlled spinodal decomposition in coherent bulk[13,14] and thin film systems [two dimensional (2D) and three dimensional (3D)] have been studied.[15,16] In the present paper, we employ a phase-field model of diffusionless phase separation for description of morphology of nanostructures in constrained films. This model is verified by comparing the results of simulations to the observed morphologies of multiferroic nanostructures in the $PbTiO_3$-$CoFe_2O_4$ films grown on $SrTiO_3$ substrates having different crystallographic orientations. According to our results, the morphology strongly depends on in-plane elastic

anisotropy of the nanostructure which is determined by crystallographic orientation of the film.

Elastic interactions arise in multiphase nanostructures due to epitaxy, resulting in formation of coherent or semicoherent interphase boundaries and film/substrate interfaces. The stress state in the coherent multiphase film/substrate system can be described using the self-strains of the component phases, as determined from the differences in the lattice parameters of the undistorted phases and a substrate, the latter being used as a reference state.[11,12] For example, a coherent two-phase nanostructure consisting of $PbTiO_3$ (a_1=3.96 Å) and $CoFe_2O_4$ (a_2=8.38 Å/2=4.19 Å) on a $SrTiO_3$ (a_s=3.95 Å) substrate can be described by a distorted cubic lattice [Figs. 1(a) and 1(b)]. Since both phases are cubic at the growth temperature, the self-strains correspond to a pure dilatation, $\varepsilon_1=(a_1-a_s)/a_s=0.0025$ and $\varepsilon_2=(a_2-a_s)/a_s=0.061$. Equilibrium nanostructures which consist of coherent phases have been considered in Ref. 17. However, the nanostructures grown experimentally[1,5] are semicoherent and feature misfit dislocations [Figs. 1(c)–1(f)]. Therefore, the strain relaxation along the interfaces (both interphase boundaries and
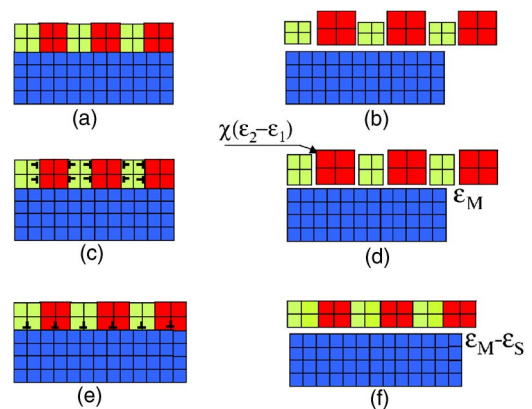
FIG. 1. (Color online) Schematic drawings of (a)–(b) a coherent two-phase structure on a substrate, (c)–(d) semicoherent structure with the interphase boundaries partially relaxed along the normal to the substrate, (e)–(f) semicoherent structure with a partially relaxed film/substrate interface.
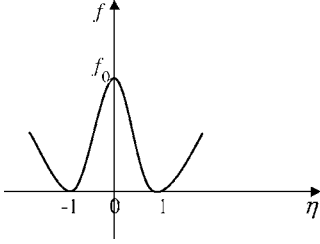
FIG. 2. Double-well potential $f(\eta)$ used in the simulations of the two-phase nanostructures.

film/substrate interface) needs to be considered. The relaxation along the interphase boundaries occurs during deposition preferentially in a direction normal to the substrate [Figs. 1(c) and 1(d)], since the relaxation parallel to the substrate is limited by the small lateral scale of the component phases (typically <50 nm). In such partially-relaxed systems, the difference between the self-strains of the phases in a film acquires a tetragonal symmetry:

$$\Delta\varepsilon = \varepsilon_0 \begin{pmatrix} 1 & 0 & 0 \\ 0 & 1 & 0 \\ 0 & 0 & \chi \end{pmatrix}; \quad \chi = 1 - \frac{b\rho}{\varepsilon_0}, \quad (1)$$

where $\varepsilon_0 = \varepsilon - \varepsilon_2$, $\chi < 1$ is a relaxation parameter, and ρ is a misfit dislocation density at the interfaces normal to the substrate with the effective Burgers vector $b = a_2 - a_1$. The final film thicknesses (>200 nm) typically exceed the critical values needed for formation of misfit dislocations so that the film/substrate interface becomes semicoherent [Figs. 1(e) and 1(f)] which results in the relaxation of the average stresses in the film. This relaxation can be described by an effective change in the substrate lattice parameter, $a_s^{eff} = a_s(1 - \rho_m b)$, where ρ_m is the misfit dislocation density and b is the dislocation Burgers vector.[18,19]

Near equilibrium, the arrangement of phases, their morphologies, and the relaxation parameters of the interfaces (χ, a_s^{eff}) can be found by minimizing the sum of the elastic and interfacial energies for a given phase fraction. Since for the equilibrium semicoherent systems, the phase fraction is explicitly related to the relaxation parameters, phase-field modeling which assumes fixed values of the relaxation parameters can be used to find the equilibrium morphologies and phase fractions for semicoherent nanostructures.

In the phase-field model, a multiphase system is described as a continuous field of the order parameter, $\eta(\mathbf{r})$. Unconstrained equilibrium phases correspond to the two minima (η_0^1, η_0^2) of the specific free energy $f(\eta)$ (Fig. 2). The self-strain is a linear function of the order parameter:

$$\varepsilon_{ij}^0(\mathbf{r}) = \varepsilon_{ij}^0 \cdot \eta(\mathbf{r}) + \bar{\varepsilon}_{ij}^0 \quad (2)$$

which yields the self-strains of equilibrium phases ε_1 and ε_2 at $\eta = \eta_0^1$ and $\eta = \eta_0^2$, respectively. Assuming $\eta_0^1 = 1$ and $\eta_0^2 = -1$ (Fig. 2) the self-strain for the PbTiO$_3$-CoFe$_2$O$_4$ films on SrTiO$_3$ is

$$\varepsilon_{ij}^0(\mathbf{r}) = \frac{1}{2}\varepsilon_0 \begin{pmatrix} 1 & 0 & 0 \\ 0 & 1 & 0 \\ 0 & 0 & \chi \end{pmatrix} \cdot \eta(\mathbf{r}) + \bar{\varepsilon}_0 \begin{pmatrix} 1 & 0 & 0 \\ 0 & 1 & 0 \\ 0 & 0 & 1 \end{pmatrix}, \quad (3)$$

where $\varepsilon_0 = (\varepsilon_1 - \varepsilon_2) = -0.058$, $\bar{\varepsilon}_0 = (\varepsilon_1 + \varepsilon_2)/2 = 0.031$. Then, the equilibrium two-phase nanostructure can be determined by minimizing the free energy functional along $\eta(\mathbf{r})$:

$$F = \int_V \left[f(\eta) + \frac{1}{2}\beta_{ij}\frac{\partial\eta}{\partial x_i}\frac{\partial\eta}{\partial x_j} + \frac{1}{2}C_{ijkl}(\varepsilon_{ij}(\mathbf{r}) - \varepsilon_{ij}^0(\mathbf{r}))(\varepsilon_{kl}(\mathbf{r}) \right.$$
$$\left. - \varepsilon_{kl}^0(\mathbf{r})) \right] dV. \quad (4)$$

The first and second terms in the integrand determine the interfacial energy, where β_{ij} is a gradient coefficient. The third term represents elastic energy, where C_{ijkl} is the elastic modulus, $\varepsilon_{ij}(\mathbf{r})$ denotes total strain, and $\varepsilon_{ij}^0(\mathbf{r})$ is the transformation self-strain. The order parameter of the substrate, η_S, is fixed. Since $\varepsilon_{s_{ij}}^{eff} = \frac{a_s^{eff} - a_s}{a_s} = \varepsilon_{ij}^0 \cdot \eta_s + \bar{\varepsilon}_{ij}^0$, the value of η_S describes the relaxation of the film/substrate interface.

The phase fractions, periodicity, and arrangement in the equilibrium nanostructure can be obtained for any given relaxation parameters, η_s and χ, using

$$\frac{\delta F}{\delta\eta(\mathbf{r})} = 0, \quad (5)$$

where $\delta \cdots / \delta\eta(\mathbf{r})$ is a variational derivative. To solve Eq. (5), we use the relaxation procedure, which considers a virtual phase transformation from the unstable initial phase ($\eta = 0$) to a two-phase state corresponding to the two minima of $f(\eta)$. The function

$$f(\eta) = f_0(1 - \eta^2)^2 \quad (6)$$

satisfies these conditions with the minima at $\eta_0^1 = -1$, $\eta_0^2 = 1$. The time evolution of the phase-field of the order parameter $\eta[r(t)]$ is described by the equation:

$$\frac{\partial\eta}{\partial t} = -L\frac{\delta F}{\delta\eta} + \xi, \quad (7)$$

where L is a kinetic coefficient and ξ is the Langevin noise term. To solve Eq. (7) we use Khachaturyan's microelasticity approach in phase-field modeling.[17,20,21]

For simplicity, an elastically homogeneous medium is assumed. Since the elastic anisotropy $\left(\varsigma = \frac{C_{11} - C_{12} - 2 \cdot C_{44}}{C_{44}} \right)$ of cubic PbTiO$_3$ is relatively small,[22] whereas the elastic anisotropy of CoFe$_2$O$_4$ is significantly positive ($\xi = 0.5$),[23] the positive average anisotropy ($\xi = 0.3$) is used for modeling. The self-strain describing the difference between the lattice parameters of the two phases is $\varepsilon_0 = -0.058$. The relaxation along the interphase boundaries, χ, is assumed to be constant and determined by $\chi = 0.2 - 0.8$, which corresponds to the linear densities of interfacial dislocations ($\rho = 8 \times 10^8 - 4 \times 10^7$ cm^{-1}).

The orientational dependence of the interfacial energy was neglected in comparison with that of the elastic energy, so that $\beta_{ij} = \beta\delta_{ij}$ (δ_{ij} is a Kronecker symbol). The parameter

$\beta = 0.5 e_0 l_0^2$ determines the interfacial energy $\Gamma = e_0 l_0$, where $e_0 = \frac{1}{2} C_{iklm} \varepsilon_{ik}^0 \varepsilon_{lm}^0$ is a characteristic energy and l_0 is the length of a computational grid cell. Different crystallographic orientations of the film were introduced by rotating the elastic moduli tensor $C_{ijjk}, C_{mnop} = a_{mi} a_{nj} a_{ok} a_{pl} C_{ijkl}$, $a_{\alpha\beta}$ are the rotation matrix elements. Three different orientations of the substrate were considered; (001), (110), and (111).

The $64 \times 64 \times 64$ mesh of a computational volume with periodical boundary conditions consisting of active (film) and passive (substrate) layers is used for the simulations. The relative thickness of the film, $\gamma = 3/8$, corresponds to a film thickness of about 200 nm. The simulation of the composite structure with alternating active and passive layers provides an adequate description of the structure formation in the film if the nanostructure periodicity is smaller than the film thickness.[20] Transformation from an unstable initial state occurs via nucleation of the stable phases as driven by the Langevin noise in the time evolution equation. After a sufficiently long relaxation process equilibrium between the two phases is established.

Analysis of the simulation results reveals that the volume fractions of the component phases are determined by the relaxation parameter, η_s. For the film thickness used in the simulations the effective misfit between the film and the substrate is close to zero and the average stress due to the film/substrate interactions is almost completely relaxed. A similar relaxed state is established in a constrained film consisting of the twin-type elastic domains representing different orientational variants of the same phase.[24–27] The dependence of the domain fraction on film/substrate misfit was considered analytically in[25–27] and numerically in.[24] In contrast to the twin-type domains, the individual phases in a multiphase film are incompatible, and, therefore, the interphase boundaries generate internal stresses. The orientational dependence of the elastic energy associated with these stresses dictates the morphological features of multiphase nanostructures. According to our simulations, the dependence of the elastic energy on the relaxation parameter, χ, is weak, because the changes in χ affect only a relatively small part of the elastic energy. The periodicity of the nanostructures, D, is much larger than the interface thickness, l_0; therefore, the elastic energy per domain $D e_0$ is much larger than the interfacial energy $\Gamma = e_0 l_0$. The morphologies of the simulated structures are thus dominated by the elastic rather than by the interfacial energy.

The nanostructures computed for $\chi = 0.4$ in the films having (001), (110), and (111) orientations are presented in Fig. 3. The interphase boundaries in all structures are perpendicular to the substrate surface. According to the simulations, the dissimilar in-plane morphologies in differently oriented films are determined by the in-plane elastic anisotropy of the film which varies with the film/substrate orientation.

The validity of the theoretical modeling was verified by comparison with the observed epitaxial $CoFe_2O_4$-$PbTiO_3$ nanostructures grown from a composite $0.67PbTiO_3$-$0.33CoFe_2O_4$ and $0.33PbTiO_3$-$0.67CoFe_2O_4$ targets using pulsed-laser deposition (PLD). $SrTiO_3$ single crystals having (001), (110), and (111) orientations were used as substrates. The films with a thickness of 230 nm were deposited simultaneously on the differently oriented substrates to ensure similar growth conditions. The substrate temperature during
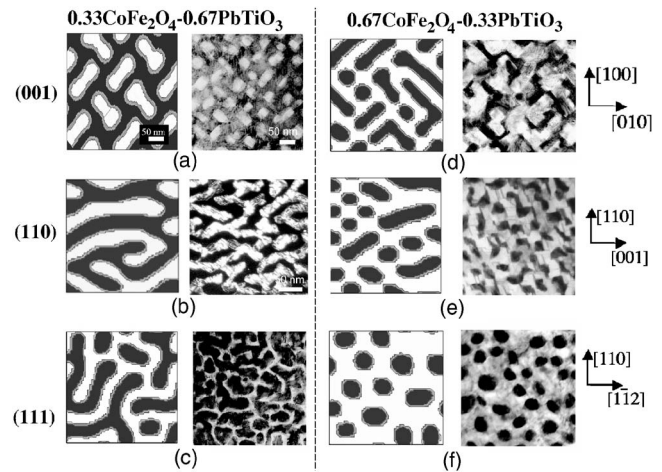
FIG. 3. Top view of nanostructure morphologies in the epitaxial $0.33CoFe_2O_4$-$0.67PbTiO_3$ (a)–(c) and $0.67CoFe_2O_4$-$0.33PbTiO_3$; (e)–(f) films grown on $SrTiO_3$ substrates having (a), (d)–(001), (b), (e)–(110), and (c), (f)–(111) orientations. Two images are shown for each combination of composition and orientation. The images on the left are results of the phase-field modeling, whereas the images on the right are experimental TEM micrographs. In all the images, the $CoFe_2O_4$ and $PbTiO_3$ phases appear as *bright* and *dark* regions, respectively.

deposition was kept at 630 °C. The samples were examined in a transmission electron microscope operated at 200 kV.

Regardless of substrate orientation, cube on cube 3D epitaxial growth of the two-phase $CoFe_2O_4$-$PbTiO_3$ films was obtained with interphase boundaries oriented perpendicular to the film/substrate interface. However, the nanostructure morphologies varied markedly with the substrate orientation and film composition (Fig. 3). In particular, for the $PbTiO_3$-rich composition, isolated vertical nanorods/nanoplates of $CoFe_2O_4$ faceted on {110} planes [Fig. 3(a)] are obtained on an (001) substrate, whereas vertical $CoFe_2O_4$ nanoplates faceted on {111} planes [Fig. 3(c)] are obtained on a (110) substrate; these {111} nanoplates merge to form two sets of stripes preferentially ($\pm 35°$) aligned along the in-plane [100] direction [Fig. 3(c)]. The labyrinthlike nanostructure of the $PbTiO_3$-rich films grown on (111) substrates [Fig. 3(e)] transforms into well-organized $PbTiO_3$ nanorods embedded in a $CoFe_2O_4$ matrix with increasing fraction of the $CoFe_2O_4$ phase [Fig. 3(f)]. According to our results, nanostructures containing isolated magnetic nanorods in a ferroelectric matrix [Fig. 3(a)] or vice versa [Fig. 3(f)] can be obtained by varying the substrate orientation and phase fraction. Comparison of the simulated and experimental nanostructures (Fig. 3) demonstrates that our phase-field modeling successfully reproduced even fine morphological details observed in the experimentally grown films and suggests that this approach can be used to predict the architecture of multiferroic nanostructures.

Despite a good agreement between the simulated and experimental nanostructure morphologies, their lateral scale is different. Possibly, the scale in the experimental nanostructures is determined by the growth conditions (e.g., temperature, growth rate) rather than by the elastic interactions; that is, the scale experimentally observed is diffusion limited and

does not represent the equilibrium. Alternatively, the scale in our calculations may not represent the true equilibrium periodicity because information on the energies of the interphase boundaries is lacking. Further experiments (for example, using higher growth temperatures) are needed to clarify this issue.

The nanostructures corresponding to different film orientations are expected to exhibit remarkably different functional properties. For the $CoFe_2O_4$-$PbTiO_3$ system, a large tetragonal strain in $PbTiO_3$ causes dramatic changes in the stress state due to different misfits with differently oriented substrates.[28] Consequently, the magnetic and dielectric properties of $CoFe_2O_4$-$PbTiO_3$ nanostructures depend strongly on a substrate orientation.[7] The dominant mechanism of interphase coupling can also vary for differently oriented films depending on the orientation of electric polarization and magnetization with respect to the nanostructure. For example, for the (001) orientation, where both polarization and magnetization are parallel to the substrate normal, the coupling should be determined by the elastic interactions. In contrast, for other orientations with either polarization and/or magnetization being inclined to the interphase boundaries, the interphase coupling can involve different mechanisms due to the significant electric and/or magnetic charges generated at these interfaces. The analysis of these interactions

and their effect on both magnetic and electrical response is the subject of our future studies.

In summary, the thermodynamic model, which treats dissimilar nanophases in an epitaxial film as elastic domains, is presented to explain the morphology of self-assembling heterophase nanostructures forming during film deposition. The model successfully predicts and reproduces complex morphologies and their dependence on film orientations and phase fractions for multiferroic $CoFe_2O_4$-$PbTiO_3$ nanostructures grown on differently oriented $SrTiO_3$ substrates. The good agreement between the results of the modeling and experimental observations confirms that the morphology of investigating nanostructures is close to an equilibrium one, which is dominated by elastic interactions between nanostructure components. It allows us to conclude that under appropriate deposition conditions, elastic interactions play an important role in the formation of self-assembling nanostructures in epitaxial films. Control of these interactions may lead to the theoretical design of multifunctional nanostructures with optimal properties.

[1] H. Zheng, J. Wang, S. E. Lofland, Z. Ma, L. Mohaddes-Ardabili, T. Zhao, L. Salamanca-Riba, S. R. Shinde, S. B. Ogale, F. Bai, D. Viehland, Y. Jia, D. G. Schlom, M. Wuttig, A. Roytburd, and R. Ramesh, Science **303**, 661 (2004).

[2] H. Zheng, J. Wang, L. Mohaddes-Ardabili, M. Wuttig, L. Salamanca-Riba, D. G. Schlom, and R. Ramesh, Appl. Phys. Lett. **85**, 2035 (2004).

[3] J. Wang, H. Zheng, Z. Ma, S. Prasertchoung, M. Wuttig, R. Droopad, J. Yu, K. Eisenbeiser, and R. Ramesh, Appl. Phys. Lett. **85**, 2574 (2004).

[4] C.-W. Nan, G. Liu, Y. Lin, and H. Chen, Phys. Rev. Lett. **94**, 197203 (2005).

[5] M. Fiebig, J. Phys. D **38**, R123 (2005).

[6] N. Hur, S. W. Cheong, S. N. Kale, S. B. Ogale, R. Choudhary, S. R. Shinde, and T. Venkatesan, Appl. Phys. Lett. **86**, 112507 (2005).

[7] J. Li, I. Levin, J. Slutsker, V. Provenzano, P. K. Shenk, R. Ramesh, J. Ouyang, and A. L. Roytburd, Appl. Phys. Lett. **87**, 072909 (2005).

[8] M. I. Bichurin, V. M. Petrov, and G. Srinivasan, J. Appl. Phys. **92**, 7681 (2002).

[9] M. I. Bichurin, V. M. Petrov, and G. Srinivasan, Phys. Rev. B **68**, 054402 (2003).

[10] G. Srinivasan, E. T. Rasmussen, B. Levin, and R. Hayes, Phys. Rev. B **65**, 134402 (2002).

[11] A. L. Roitburd, Phys. Status Solidi A **37**, 329 (1976).

[12] A. L. Roytburd, J. Appl. Phys. **83**, 238 (1998).

[13] C. Sagui, D. Orlikowski, A. M. Somoza, and C. Roland, Phys. Rev. E **58**, R4092 (1998); D. Orlikowski, C. Sagui, A. Somoza, and C. Roland, Phys. Rev. B **59**, 8646 (1999); D. Orlikowski, C.

Sagui, A. M. Somoza, and C. Roland, *ibid.* **62**, 3160 (2000).

[14] P. Fratzl, O. Penrose, and J. L. Lebowitz, J. Stat. Phys. **95**, 1429 (1999).

[15] W. Lu and Z. Suo, J. Mech. Phys. Solids **49**, 1937 (2001).

[16] D. J. Seol, S. Y. Hu, Y. L. Li, J. Shen, K. H. Oh, and L. Q. Chen, Acta Mater. **51**, 5173 (2003).

[17] A. Artemev, J. Slutsker, and A. L. Roytburd, Acta Mater. **53**, 3425 (2005).

[18] J. S. Speck and W. Pompe, J. Appl. Phys. **76**, 466 (1994).

[19] S. P. Alpay and A. L. Roytburd, J. Appl. Phys. **83**, 4714 (1998).

[20] A. G. Khachaturyan, *Theory of Structural Transformations in Solids* (John Wiley & Sons, New York, 1983).

[21] A. Artemev, Y. Jin, and A. G. Khachaturyan, Acta Mater. **49**, 1165 (2001).

[22] B. D. Chapman, E. A. Stern, S.-W. Han, J. O. Cross, G. T. Seidler, V. Gavrilyatchenko, R. V. Vedrinskii, and V. L. Kraizman, Phys. Rev. B **71**, 020102(R) (2005).

[23] Z. Chen, S. Yu, L. Meng and Y. Len, Compos. Struct. **75**, 177 (2002).

[24] J. Slutsker, A. Artemev, and A. L. Roytburd, Acta Mater. **52**, 1731 (2004).

[25] A. M. Bratkovsky and A. P. Levanyuk, Phys. Rev. Lett. **86**, 3642 (2001).

[26] A. M. Bratkovsky and A. P. Levanyuk, Phys. Rev. B **65**, 094102 (2002).

[27] A. M. Bratkovsky and A. P. Levanyuk, Phys. Rev. B **66**, 184109 (2002).

[28] J. Ouyang, S. Y. Yang, L. Chen, R. Ramesh, and A. L. Roytburd, Appl. Phys. Lett. **85**, 278 (2004).